

Federated Beamforming with Subarrayed Planar Arrays for B5G/6G LEO Non-Terrestrial Networks

*Original*

Federated Beamforming with Subarrayed Planar Arrays for B5G/6G LEO Non-Terrestrial Networks / Dakkak, M. R.; Riviello, D. G.; Guidotti, A.; Vanelli-Coralli, A.. - ELETTRONICO. - (2024), pp. 1-6. (Intervento presentato al convegno 25th IEEE Wireless Communications and Networking Conference, WCNC 2024 tenutosi a Dubai (United Arab Emirates) nel 21-24 April 2024) [10.1109/WCNC57260.2024.10571202].

*Availability:*

This version is available at: 11583/2991741 since: 2024-08-17T10:58:43Z

*Publisher:*

IEEE

*Published*

DOI:10.1109/WCNC57260.2024.10571202

*Terms of use:*

This article is made available under terms and conditions as specified in the corresponding bibliographic description in the repository

*Publisher copyright*

IEEE postprint/Author's Accepted Manuscript

©2024 IEEE. Personal use of this material is permitted. Permission from IEEE must be obtained for all other uses, in any current or future media, including reprinting/republishing this material for advertising or promotional purposes, creating new collecting works, for resale or lists, or reuse of any copyrighted component of this work in other works.

(Article begins on next page)

# Federated Beamforming with Subarrayed Planar Arrays for B5G/6G LEO Non-Terrestrial Networks

M. Rabih Dakkak\*, Daniel Gaetano Riviello\*, Alessandro Guidotti<sup>†</sup>, Alessandro Vanelli-Coralli\*

\*Dept. of Electrical, Electronic, and Information Engineering (DEI), Univ. of Bologna, Bologna, Italy

<sup>†</sup>National Inter-University Consortium for Telecommunications (CNIT), Bologna, Italy

{mrabih.dakkak2, daniel.riviello, a.guidotti, alessandro.vanelli}@unibo.it

**Abstract**—Non-Terrestrial Networks (NTNs) will be an essential element in Beyond-5G (B5G) and 6G ecosystems, with the purpose of enabling seamless and global coverage, as well as supporting high data rate services. To achieve that, Full Frequency Reuse (FFR) schemes, along with digital beamforming techniques to cope with the Co-Channel Interference (CCI), are considered as promising strategies in 6G NTN. In this paper, we address the design of Cell-Free (CF) MIMO algorithms in NTN composed of multiple swarms of Non-GeoSynchronous Orbit (NGSO) nodes, in which each swarm performs distributed digital beamforming schemes. Furthermore, aiming at increasing the directivity of on-board antenna arrays for each NGSO node and enhancing the interference mitigation, we propose a Limited Field of View (LFoV) planar array architecture built up of smaller planar subarrays. We evaluate the performance of distributed beamforming schemes including both Channel State Information (CSI)-based, e.g., digital Minimum Mean Square Error (MMSE), and position-based such as analog Conventional Beamforming (CBF). We provide a numerical analysis of the performance in terms of per-user spectral efficiency. The results show that our proposed subarrayed architecture designed for federated CF-MIMO beamforming outperforms the reference approach without subarraying in the proposed NTN system architecture.

**Index Terms**—6G, federated MIMO, NTN, B5G, mega constellation, subarrays

## I. INTRODUCTION AND MOTIVATION

In the recent years, telecommunication networks have faced an unparalleled demand for higher capacity and the challenge of accommodating a wide range of services that have different performance needs in terms of data rate and delay. All the efforts are being made to improve 5G services through the development of new features in 5G-Advanced (5G-A) and ongoing research in 6G technologies, which will support a fully connected world, characterised by the convergence of the physical, human, and digital domains [1]. Within NTN, current Geostationary Earth Orbit (GEO) High Throughput Satellite (HTS) systems provide hundred of Gbps through multi-beam coverage [2]. These systems are based on multi-colour, e.g., 3 or 4 colours, frequency reuse schemes in which the available bandwidth is split into multiple non-overlapping spectrum chunks to limit the interference. Moreover, Low Earth Orbit (LEO) mega-constellations, which can significantly reduce the propagation delay, have received a remarkable interest, e.g., SpaceX has already planned approximately 12,000 LEO satellites; such increased visibility paves the way for implementing of advanced techniques to manage the interference [3]. As the current physical layer (PHY) technologies have

effectively reached the Shannon limit in terms of spectral efficiency, upcoming NTN systems are focusing on designing strategies that maximize the utilization of the spectrum. The reduction of the frequency reuse factor to Full Frequency Reuse (FFR) can help achieve this goal. Significantly, effective interference management techniques such as beamforming (BF), precoding, and CF-MIMO, will be utilized along with the former schemes to reduce the Co-Channel Interference (CCI). Over recent years, the implementation of beamforming techniques in NTN has been thoroughly addressed [4]–[10], focusing on enhancing the system throughput in different scenarios, including unicast or multicast transmissions, ideal and non-ideal Channel State Information (CSI) knowledge at the transmitter, GeoSynchronous Orbit (GSO) and, more recently, Non-GeoSynchronous Orbit (NGSO) systems, and advanced Radio Resource Management (RRM) algorithms. In [4], the authors provide a detailed survey on the application of MIMO techniques over satellite channels: both fixed and mobile satellite communications are addressed, and the most impacting channel impairments are identified. In [11], [12], the authors propose a LEO satellite architecture based on distributed massive MIMO (DM-MIMO) technology which allows on-ground user terminals to be connected to a cluster of satellites. Moreover, this work focuses on an optimized cross-layer design framework in which the power allocation and handover management processes are jointly optimized in a DM-MIMO scenario. In [13], the authors introduce a thorough explanation of the latest developments in antenna technology that have made planar arrays suitable for commercial use in SatCom. Despite the superior benefits that phased arrays offer in terms of size, adaptable directionality, and quick configuring when compared to conventional techniques like parabolic antennas, there are still a few challenges that need to be overcome. These include the cost-effectiveness of the antenna, as well as the complexity of the Beamforming Network (BFN), power efficiency, and an increasing number of antenna elements needed to meet the high demands of B5G/6G systems. To properly address such complexity and cost issues, subarraying is introduced as one of the main solutions in [14], and has been implemented in MU-MIMO in [15]. Moreover, a novel beamforming architecture based on phased subarrays is proposed in [16] for Terrestrial Networks (TNs). This study showed that subarrays, when properly combined at the user locations, provide relatively high gains towards the intended

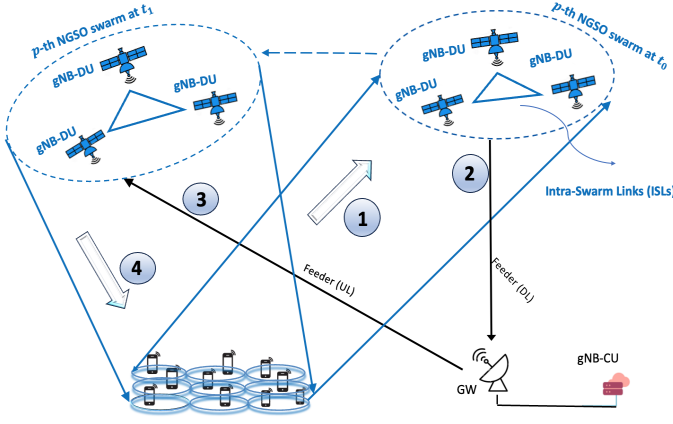


Fig. 1: System architecture for  $p$ -th NGSO swarm in NTN.

users and sufficiently low inter-user interference levels. In [17], the authors introduce the architecture of Limited Field of View (LFoV) arrays that utilize narrow steering angular range, in which subarrays can be placed at a spacing greater than half of the wavelength to increase the directivity towards the target user. Although such spacing beyond half of the wavelength could potentially cause grating lobes, however these lobes would appear outside the narrow steering range and will not impact the performance of this type of application.

In this paper, we propose NTN architecture composed of multiple swarms of NGSO nodes, each swarm implements Cell-Free (CF) MIMO algorithms based on federated beamforming schemes. Additionally, we incorporate a Limited Field of View (LFoV) planar array of subarrays design on-board of each node. To the best of our knowledge, the incorporation of CF-MIMO with LFoV subarrays into such type of NTN architectures, has not been proposed yet in literature. This research builds upon and extends the analysis presented in our recent works in [18], [19]. The remainder of the work is the following: Sec. II outlines the system model description and the assumptions, Sec. III introduces the proposed beamforming schemes both those based on CSI or users' positions. The numerical results and discussion are presented in Sec. IV, and finally, Sec. V concludes the contribution and the possible future works.

#### A. Notation

In the paper, unless stated otherwise, the utilized notation is as follows: vectors are represented by bold lowercase letters and matrices by bold uppercase letters.  $\mathbf{A}^T$  and  $\mathbf{A}^H$  denote the transpose and the conjugate transpose of  $\mathbf{A}$ , respectively.  $\mathbf{A}_{i,:}$  and  $\mathbf{A}_{:,i}$  refer to the  $i$ -th row and the  $i$ -th column of matrix  $\mathbf{A}$ , respectively. Finally,  $\text{tr}(\mathbf{A})$  denotes the trace of matrix  $\mathbf{A}$ .

### II. SYSTEM MODEL

We consider a constellation of NGSO nodes providing the service to the on-ground User Equipments (UEs). Notably, for a generic coverage area, only a subset of nodes will be visible from all of the UEs, based on the nodes' field of view and on minimum elevation angle requirements. In this

paper, we assume  $S$  nodes in a single swarm are visible by the UEs in the considered area. The visibility assumption is possible thanks to the handover procedure that can be implemented through Intra-Swarm Links (ISLs) and/or Inter-Swarm links in the constellation [11]. It is worth mentioning that the handover procedure is out of scope of this paper where the focus will be on the analysis of cell free federated MIMO schemes within swarms of multiple satellites. Thanks to ISLs, the nodes synchronize the transmission in the time and frequency domains for realization of distributed BF schemes in feed space scenario.

Each node is equipped with an on-board Uniform Planar Array (UPA) made of  $N_{tot} = MN$  total radiating elements grouped into  $N$  subarrays of  $M$  elements, providing connectivity to  $K$  uniformly distributed on-ground UEs and utilizing the same spectral resources (FFR). We consider (according to 3GPP) Earth-moving beams, i.e., the coverage area of each node is always centered around its Sub Node Point (SNP) and, thus, the beams move on-ground along with the node on its orbit. For the sake of simplicity, we assume that all the nodes are at the same altitude and are equipped with the same antenna configuration as a typical mega-constellation. To ensure the user connectivity, the NGSO node shall establish a logical connection with a Centralized Unit on-ground gNB-CU. To achieve this, each node is presumed to be directly linked to a ground-based gateway (GW), or to be connected to another node in the constellation by means of ISLs. It is worth mentioning that the adopted system architecture of NGSO constellation is thoroughly described in [20]. Fig. 1 depicts the system architecture of the  $p$ -th NGSO swarm which requires  $G$  on-ground GWs but for sake of clarity we depict only one GW. The nodes are supposed to enable BF schemes, detailed in the next section, which require the estimates of either the CSI or the user locations to be provided by the UEs. Fig. 1 also illustrates the four main steps of on-ground BF in the proposed scenario: i) the CSI or location estimates are obtained by the UEs at time instant  $t_0$  and sent to the network, when the nodes of the  $p$ -th swarm are located at a specific orbital position; ii) the estimates are returned to the gNB-CU to calculate the beamforming coefficients; iii) such coefficients are sent to the nodes of the  $p$ -th swarm to be applied to the users' signals on-board by each gNB-DU (Distributed Unit); iv) the transmission of the beamformed signals occurs at time instant  $t_1 > t_0$ . During the aging interval,  $\Delta t = t_1 - t_0$ , the NGSO nodes have moved and, thus, there is a misalignment between the actual channel used during the transmission and the estimated channel used to compute the beamforming matrix. Hence, the MIMO performance will be impacted by such misalignment; the smaller the aging delay, the better the MIMO performance. The aging delay is computed as:

$$\Delta t = t_{user} + t_{feeder}^{(UL)} + t_{feeder}^{(DL)} + t_p + t_{rout} + t_{ad} \quad (1)$$

where: i)  $t_{user}$  is the latency on the user return link; ii)  $t_{feeder}^{(DL)}$  is the delay on the feeder downlink; ii)  $t_{feeder}^{(UL)}$  is the delay on the feeder uplink; iii)  $t_p$  is the processing delay required to compute the beamforming coefficients; and iv)

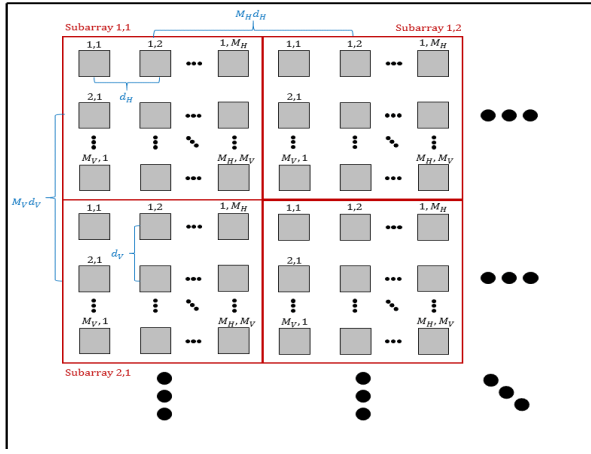


Fig. 2: Structure of the subarrayed UPA of the  $s$ -th node.

$t_{\text{rout}}$  is the latency due to routing on the ISLs, if present; finally  $t_{\text{ad}}$  includes any additional delay (e.g., large scale loss, scintillation, etc.). Moreover, to avoid the feeder link latency, beamforming procedure could be implemented totally on-board to mitigate the channel aging issue.

The antenna array model for each node is based on ITU-R Recommendation M.2101-0 [21]. Generally, the antenna boresight direction points to the SNP, while the point  $P$  represents the position of the user terminal on the ground. The user direction can be identified by the angle pair  $(\vartheta, \varphi)$  where the boresight direction is  $(0,0)$ . We can now derive the direction cosines for the considered user as:  $u = \frac{P_y}{\|P\|} \sin \vartheta \sin \varphi$ , and  $v = \frac{P_z}{\|P\|} \cos \vartheta$ . The total array response of the UPA of the  $s$ -th node in the generic direction  $(\vartheta_{i,s}, \varphi_{i,s})$  can be expressed as the Kronecker product between the array responses of the 2 Uniform Linear Arrays (ULAs) of the  $s$ -th node lying on the  $y$ -axis and  $z$ -axis. We first define the  $1 \times N_H$  Steering Vector (SV) of the ULA along the  $y$ -axis,  $\mathbf{a}_H(\vartheta_{i,s}, \varphi_{i,s})$ , and the  $1 \times N_V$  SV of the ULA along the  $z$ -axis,  $\mathbf{a}_V(\vartheta_{i,s})$  [22]:

$$\mathbf{a}_H(\vartheta_{i,s}, \varphi_{i,s}) = [1, e^{jk_0 M_H d_H \sin \vartheta_{i,s} \sin \varphi_{i,s}}, \dots, e^{jk_0 M_H d_H (N_H - 1) \sin \vartheta_{i,s} \sin \varphi_{i,s}}] \quad (2)$$

$$\mathbf{a}_V(\vartheta_{i,s}) = [1, e^{jk_0 M_V d_V \cos \vartheta_{i,s}}, \dots, e^{jk_0 M_V d_V (N_V - 1) \cos \vartheta_{i,s}}] \quad (3)$$

where:  $k_0 = 2\pi/\lambda$  is the wave number,  $N_H, N_V$  denote the number of subarrays on the horizontal and vertical directions, respectively, with  $N = N_H N_V$ , and  $M_H, M_V$  denote the number of antenna elements per each subarray on the horizontal ( $y$ -axis) and vertical ( $z$ -axis) directions, respectively, with  $M = M_H M_V$ , and finally  $d_H, d_V$  denote the distance between adjacent antenna elements on the horizontal and vertical directions, respectively, as shown in Fig. 2. It is worth mentioning that the total number of antenna elements for each  $s$ -th node are  $N_{\text{tot}} = MN$ , where  $M = 1$ , if subarraying is not implemented. We can define the total steering vector of the full UPA (an array equipped with subarrays as antenna elements) of the  $s$ -th node as the Kronecker product of the 2 SV's along each axis:

$$\mathbf{a}_{\text{UPA}}(\vartheta_{i,s}, \varphi_{i,s}) = \mathbf{a}_H(\vartheta_{i,s}, \varphi_{i,s}) \otimes \mathbf{a}_V(\vartheta_{i,s}) \quad (4)$$

We further assume that the node is equipped with directive antenna elements, whose radiation pattern is denoted by  $g_E(\vartheta_{i,s}, \varphi_{i,s})$  according to Table 3 in [21], and these elements are grouped into  $N$  subarrays of size  $M_H \times M_V$ . We can define the subarray factor  $F_{\text{sub}}(\vartheta_{i,s}, \varphi_{i,s})$  as:

$$F_{\text{sub}}(\vartheta_{i,s}, \varphi_{i,s}) = \frac{\sin\left(\frac{M_V}{2} k_0 d_V \cos \vartheta_{i,s}\right)}{\sqrt{M_V} \sin\left(\frac{1}{2} k_0 d_V \cos \vartheta_{i,s}\right)} \frac{\sin\left(\frac{M_H}{2} k_0 d_H \sin \vartheta_{i,s} \sin \varphi_{i,s}\right)}{\sqrt{M_H} \sin\left(\frac{1}{2} k_0 d_H \sin \vartheta_{i,s} \sin \varphi_{i,s}\right)} \quad (5)$$

Finally, we can express the total SV of the UPA of subarrays made of directive antenna elements at the  $s$ -th node targeted towards the  $i$ -th user as the product of  $\mathbf{a}_{\text{UPA}}(\vartheta_{i,s}, \varphi_{i,s})$ , the element radiation pattern  $g_E(\vartheta_{i,s}, \varphi_{i,s})$  and the subarray factor  $F_{\text{sub}}(\vartheta_{i,s}, \varphi_{i,s})$ :

$$\mathbf{a}(\vartheta_{i,s}, \varphi_{i,s}) = g_E(\vartheta_{i,s}, \varphi_{i,s}) F_{\text{sub}}(\vartheta_{i,s}, \varphi_{i,s}) \mathbf{a}_{\text{UPA}}(\vartheta_{i,s}, \varphi_{i,s}) \quad (6)$$

The CSI vector  $\mathbf{h}_{i,s}$ , which represents the channel between the  $i$ -th on-ground UE and the UPA on-board of the  $s$ -th node, can be written as:

$$\mathbf{h}_{i,s} = G_{i,s}^{(rx)} \frac{\lambda}{4\pi d_{i,s}} \sqrt{\frac{L_{i,s}}{\kappa B T_i}} e^{-j\frac{2\pi}{\lambda} d_{i,s}} e^{-j\psi_{i,s}} \mathbf{a}(\vartheta_{i,s}, \varphi_{i,s}) \quad (7)$$

where: i)  $d_{i,s}$  is the slant range between the  $i$ -th user and  $s$ -th node; ii)  $\kappa B T_i$  denotes the equivalent thermal noise power, with  $\kappa$  being the Boltzmann's constant,  $B$  is the user bandwidth which is assumed to be the same for all users, and  $T_i$  is the equivalent noise temperature of the  $i$ -th user receiving equipment; iii)  $L_{i,s}$  denotes the additional losses between the  $s$ -th node and  $i$ -th user (e.g., atmospheric and antenna cable losses), and iv)  $G_{i,s}^{(rx)}$  denotes the receiving antenna gain for the  $i$ -th user w.r.t the  $s$ -th node and v)  $\psi_{i,s}$  is the possible misalignment between different nodes due to non-ideal swarm synchronization, modelled as a Gaussian random variable (RV). The additional losses are computed as:

$$L_{i,s} = L_{i,s}^{\text{sha}} + L_{i,s}^{\text{atm}} + L_{i,s}^{\text{sci}} + L_{i,s}^{\text{CL}} \quad (8)$$

where  $L_{i,s}^{\text{sha}}$  represents the log-normal shadow fading term,  $L_{i,s}^{\text{atm}}$  the atmospheric loss, and  $L_{i,s}^{\text{sci}}$  the scintillation, and  $L_{i,s}^{\text{CL}}$  is the Clutter Loss, to be included for the UEs in Non-Line-of-Sight (NLOS) condition. These terms are computed based on 3GPP TR 38.811 [23], in which it is also defined a Line-of-Sight (LOS) probability that is a function of the propagation environment and the elevation angle for each UE.

For the generic  $i$ -th user, its overall channel signature can be obtained by collecting the CSI vectors from all of the NGSO nodes into the  $NS$ -dimensional  $\mathbf{h}_i^{(t_0)} = [\mathbf{h}_{i,1}^{(t_0)}, \dots, \mathbf{h}_{i,S}^{(t_0)}]$ . The overall  $K \times (NS)$  channel matrix at the estimation time  $t_0$  is given by  $\hat{\mathbf{H}}_{\text{Sys}} = \left[ \left( \mathbf{h}_1^{(t_0)} \right)^T, \dots, \left( \mathbf{h}_S^{(t_0)} \right)^T \right]^T$ . For each time slot, the Radio Resource Management (RRM) algorithm selects a subgroup of  $K_{\text{sch}}$  users to be scheduled, resulting in a  $K_{\text{sch}} \times (NS)$  complex scheduled channel matrix,  $\hat{\mathbf{H}} = \mathcal{F}(\hat{\mathbf{H}}_{\text{Sys}})$  where  $\mathcal{F}(\cdot)$  stands for the RRM function.

Hence,  $\hat{\mathbf{H}} \subseteq \hat{\mathbf{H}}_{Sys}$  is defined as a sub-matrix of  $\hat{\mathbf{H}}_{Sys}$ , which only includes the rows associated with the scheduled users. The proposed BF scheme calculates the  $(NS) \times K_{sch}$  complex beamforming matrix  $\mathbf{W}$  which projects the  $K_{sch}$  dimensional column vector,  $\mathbf{s} = [s_1, \dots, s_{K_{sch}}]^T$  which contains the unit-variance user symbols, onto the  $(NS)$ -dimensional space determined by all of the swarm antenna feeds. The signal received by the generic  $i$ -th UE is given by [18]:

$$y_i = \underbrace{\mathbf{h}_i \mathbf{W}_{:,i}}_{\text{intended}} s_i + \underbrace{\sum_{k=1, k \neq i}^{K_{sch}} \mathbf{h}_i \mathbf{W}_{:,k} s_k}_{\text{interfering}} + z_i \quad (9)$$

where  $z_i$  is a circularly symmetric Gaussian RV with zero mean and unit variance. The unit variance is motivated by observing that the channel coefficients in (7) are normalised to the noise power. The  $K_{sch}$ -dimensional vector of received symbols is:

$$\mathbf{y} = \mathbf{H}_{t_1} \mathbf{W}_{t_0} \mathbf{s} + \mathbf{z} \quad (10)$$

It shall be noted that, as previously discussed, the estimated channel matrix  $\hat{\mathbf{H}}_{t_0}$ , obtained at time instant  $t_0$ , is used to compute the beamforming matrix  $\mathbf{W}_{t_0}$ , whereas, at time instant  $t_1$ , the channel matrix to be used is different and characterized by  $\mathbf{H}_{t_1}$ . From (9), the Signal-to-Interference-plus-Noise Ratio (SINR<sub>*i*</sub>) can be computed as:

$$\text{SINR}_i = \frac{\|\mathbf{h}_i \mathbf{W}_{:,i}\|^2}{1 + \sum_{k=1, k \neq i}^{K_{sch}} \|\mathbf{h}_i \mathbf{W}_{:,k}\|^2} \quad (11)$$

From the above SINR, the spectral efficiency, with which each user is served in each time frame, can be obtained through the Shannon bound formula, defined as:

$$\eta_i = \log_2(1 + \text{SINR}_i) \quad (12)$$

### III. DISTRIBUTED BEAMFORMING SCHEMES

The following CSI/location based algorithms provide the benchmark for the assessment of the performance. Please note that digital or analog beamforming is considered only at subarray level, *i.e.*, we assume that each satellite is equipped with  $N$  RF chains for both cases  $M = 1$  and  $M > 1$ .

*a) Conventional Beamforming (CBF):* or as also called beam steering. In this approach, for each  $s$ -th node the weights are generated in order to produce a phase shift to compensate the delay of the direction  $(\theta_{i,s}, \varphi_{i,s})$  of the  $i$ -th user of interest. The overall beamforming vector designed for the  $i$ -th user can be obtained by vertically concatenating the conventional beamformer at each  $s$ -node:

$$\mathbf{W}_{:,i} = \frac{1}{\sqrt{NS}} [\mathbf{a}_{\text{UPA}}(\vartheta_{i,1}, \varphi_{i,1}), \dots, \mathbf{a}_{\text{UPA}}(\vartheta_{i,S}, \varphi_{i,S})]^H \quad (13)$$

*b) Minimum Mean Square Error (MMSE):* or Regularized Zero Forcing (RZF), is designed to solve the MMSE problem as follows:

$$\mathbf{W}_{MMSE} = \arg \min_{\mathbf{W}} \mathbb{E} \|\hat{\mathbf{H}} \mathbf{W} \mathbf{s} + \mathbf{z} - \mathbf{s}\|^2 \quad (14)$$

$$\mathbf{W}_{MMSE} = \hat{\mathbf{H}}^H (\hat{\mathbf{H}} \hat{\mathbf{H}}^H + \alpha \mathbf{I}_{K_{sch}})^{-1} \quad (15)$$

where  $\hat{\mathbf{H}}$  is the estimated channel matrix at  $t_0$ . In the above equation,  $\alpha$  is a the regularisation factor, since the channel coefficients are normalised to the noise power, its optimal value is given by  $\alpha = \frac{N}{P_{t,s}}$  [24], where  $P_{t,s}$  is the available power per node in the swarm. The above formulation is computationally efficient since, notably,  $K_{sch} < NS$ .

Lastly, as explained in [7], the power normalization is a crucial aspect in beamforming as it ensures accurate consideration of the potential power output from both the NGSO node and each individual antenna. We assume that each node has the same available on-board power  $P_{t,s}$ . We can observe that the overall  $(NS) \times K_{sch}$  beamforming matrix can be divided in blocks corresponding to the single node beamforming matrices, *i.e.*,  $\mathbf{W} = [\mathbf{W}_1 \mathbf{W}_2 \dots \mathbf{W}_S]^T$  with  $\mathbf{W}_s$  denoting the  $N \times K_{sch}$  beamforming matrix of the  $s$ -th NGSO node. Therefore, we introduce the following swarm-based normalizations:

- 1) Swarm-based Sum Power Constraint (sSPC): an upper bound is imposed on the total per-node power  $P_{t,s}$ , therefore each node beamforming matrix  $\mathbf{W}_s$  can be normalized as:

$$\tilde{\mathbf{W}}_s = \frac{\sqrt{P_{t,s}} \mathbf{W}_s}{\sqrt{\text{tr}(\mathbf{W}_s \mathbf{W}_s^H)}} \quad (16)$$

This approach guarantees that the overall emitted power satisfies i)  $\|\mathbf{W}\|_F^2 = SP_{t,s}$ ; ii) each satellite emits a power  $\|\mathbf{W}_s\|_F^2 = P_{t,s}$  for  $s = 1, \dots, S$ . Clearly, this approach leads to a slight degradation in the performance, because when the normalisation is not scalar for the entire beamforming matrix  $\mathbf{W}$  leads to a loss of orthogonality in the beamforming matrix columns.

- 2) Swarm-based Maximum Power Constraint (sMPC):

$$\tilde{\mathbf{W}}_s = \frac{\sqrt{P_{t,s}} \mathbf{W}_s}{\sqrt{N \max_j [\mathbf{W}_s \mathbf{W}_s^H]_{j,j}}} \quad (17)$$

This approach ensures that the overall emitted power is still satisfying both aforementioned conditions i and ii but actually leads to lower emitted power levels, since only a single subarray per node in the swarm will transmit the maximum power.

### IV. NUMERICAL RESULTS

In this section, we report the outcomes of the numerical assessment based on the parameters reported in Table I, considering a federated MIMO architecture with  $S = 2$  nodes at the same altitude  $h_{sat} = 600$  km. Each node in the swarm generates its corresponding lattice, as shown in Fig. 3, however this leads to some overlapping beams at the border between the two lattices, *i.e.*, there are beams that have their centers inside other beams boundaries at less than -3 dB. If two users at scheduling phase are selected from such beams, they might have very similar CSI coefficients, and therefore the matricial inversion in MMSE might be ill-conditioned.

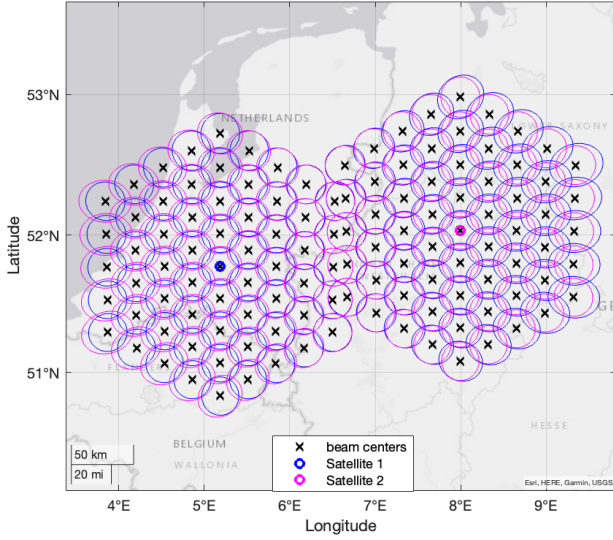


Fig. 3: Federated scenario ( $S = 2$ ). Blue lines represent the beam lattice generated by node 1 and magenta by node 2.

TABLE I: Simulation parameters.

| Parameter   | Value   |
|---|---|
| Carrier frequency   | 2 GHz   |
| System band   | S (30 MHz)  |
| Beamforming space   | feed  |
| Receiver type   | fixed VSAT  |
| Large scale scenario  | urban   |
| Propagation environment   | LOS + NLOS  |
| Number of nodes $S$ in the swarm                                | 2   |
| User density  | 0.5 user/km <sup>2</sup>  |
| Number of subarrays $N$   | 1024 ( $32 \times 32$ )   |
| Number of elements per each subarray $M$                        | ( $2 \times 2$ )<br>( $3 \times 3$ ), ( $4 \times 4$ )                |
| Number of antenna elements without Subarraying $N_{tot} = N$    | 1024  |
| Number of antenna elements with subarraying $N_{tot} = MN$      | 4096,<br>9216, 16384  |
| Number of tiers   | 4   |
| Number of scheduled users $K_{sch}$                             | 118   |
| Total per-node power density $P_{t,s,dens}$ without subarraying | 0 dBW/MHz   |
| Total per-node power density with subarraying                   | $P_{t,s,dens} - 10 \log_{10}(M_H M_V)$                                |
| Angular scanning range  | $\Delta\vartheta \simeq 37^\circ$ , $\Delta\varphi \simeq 24.5^\circ$ |

Hence, to circumvent this issue, we assume a proper RRM scheduling for the users by activating only one beam among those in which the relative distance between beam centers does not guarantee a 3 dB separation. Please notice that the beam lattices are generated only for scheduling purposes, since the aforementioned CF distributed MIMO algorithms are implemented in the feed space scenario. We assume fixed positions of UEs, and they are uniformly distributed with a density of 0.5 users/Km<sup>2</sup>. This density translates to an average number of users  $K = 37500$  to be served for each Monte Carlo iteration. The evaluation is carried out in full buffer condition, meaning that we assume unlimited traffic requirement. Based on these premises, the users are scheduled

at random. Specifically, a single user is randomly selected for each beam at each time slot, and the total number of time slots is determined to ensure that every user is served at least once. Based on the coverage area shown in Fig. 3, it is possible to compute the angular steering range for the array as  $\Delta\vartheta \simeq 37^\circ$ ,  $\Delta\varphi \simeq 24.5^\circ$  in both horizontal and vertical angular directions, respectively, which justifies the use of a LFoV array. The numerical assessment (obtained by MATLAB software) is provided for subarrayed beamforming MMSE and CBF schemes and then the performance is compared to the reference beamforming design without subarraying. In order to have a fair comparison, the transmitted power from each node, in case of subarrayed BF, has been divided by  $(M_H M_V)$ , i.e., the maximum achievable subarray gain. Hence, the Effective Isotropic Radiated Power (EIRP) for both subarrayed and non-subarrayed cases shall be equivalent. Since the LFoV array has no steering capability at antenna element level, no hybrid beamforming is taken into account. We assume a propagation scenario with both LOS and NLOS UEs (according to their LOS probability) in urban environment. Fig. 4 shows the CDFs of users' spectral efficiency for all the analyzed beamforming schemes with the sSPC and sMPC normalization considering different subarrays dimensions  $2 \times 2$ ,  $3 \times 3$  and  $4 \times 4$ . In terms of normalization, sSPC shows a slightly better performance than sMPC in all subarray configurations. It is possible to observe that both MMSE-sPC and MMSE-sMPC show the best performance with  $2 \times 2$  subarray configuration with a gain in terms of rate in the order of 7 bit/s/Hz w.r.t. the non subarrayed MMSE, whereas CBF provides the best behaviour in terms of rate (about 3.5 bit/s/Hz) with  $4 \times 4$  subarrays and it is even able to outperform MMSE with no subarrays. The superiority of the proposed subarrayed beamforming over non-subarrayed scheme, for both MMSE and CBF, is motivated by the characteristics of LFoV architecture with subarrays that enable more directive (narrower) beams towards the UEs, and, thus enhance the capability of CCI suppression.

## V. CONCLUSIONS AND FUTURE WORKS

In this work, we proposed a NTN architecture composed of multiple swarms of NGSO nodes and we assessed the performance of CF-MIMO federated CSI/location-based beamforming algorithms with LFoV antenna architecture made up of smaller planar subarrays. The numerical results provided a significant improvement in the performance in terms of spectral efficiency of the subarrayed configuration with respect to the non-subarrayed one, stating that with both configurations we have the same number of RF chains. Future works will include the design of swarm-based RRM algorithms and will consider 3D multi-layered nodes, i.e., NGSO nodes not only at the same altitude. Furthermore, Deep Learning-based CSI prediction techniques will be taken into account to address the channel aging issue in order to further improve the performance of the proposed scheme.



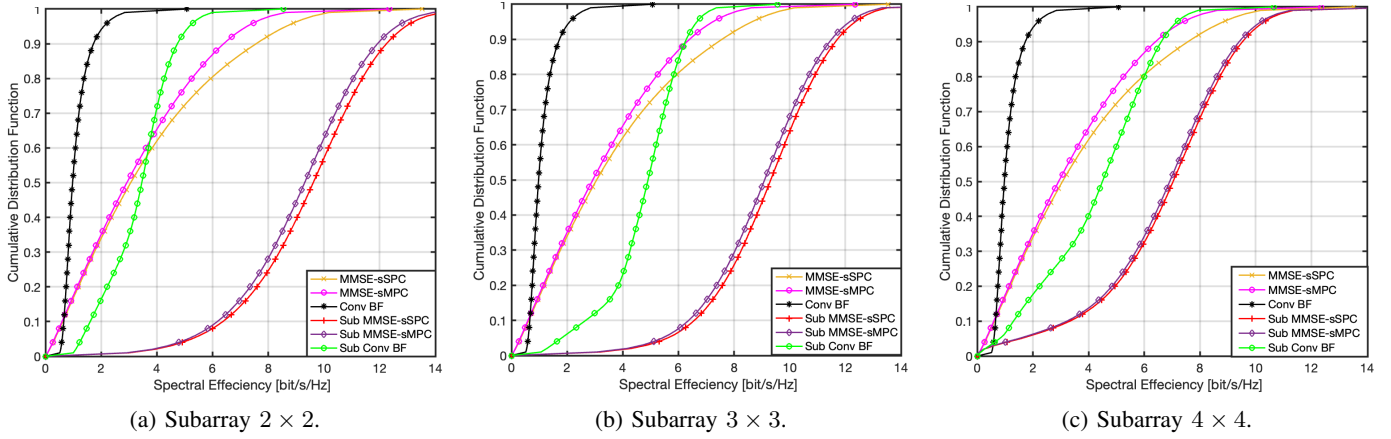


Fig. 4: CDF of users' spectral efficiency for VSATs considering different subarray configurations.

## VI. ACKNOWLEDGMENTS

This work has been funded by the 6G-NTN project, which received funding from the Smart Networks and Services Joint Undertaking (SNS JU) under the European Union's Horizon Europe research and innovation programme under Grant Agreement No 101096479. The views expressed are those of the authors and do not necessarily represent the project. The Commission is not liable for any use that may be made of any of the information contained therein.

## REFERENCES

- [1] W. Jiang, B. Han, M. A. Habibi, and H. D. Schotten, "The Road Towards 6G: A Comprehensive Survey", *IEEE Open J. Commun. Soc.*, vol. 2, pp. 334–366, 2021.
- [2] E. Feltrin, J. Freixe, and E. Weller, "Mobility in ku and ka bands: the Eutelsat's point of view," in *Proceedings of the 5th European Conference on Antennas and Propagation (EUCAP)*, 2011, pp. 2336–2340.
- [3] "Request for modification of the authorization for the SpaceX NGSO satellite system." FCC. Apr. 2021. Accessed: Jun. 2, 2022. [Online]. Available: <https://docs.fcc.gov/public/attachments/FCC-21-48A1.pdf>
- [4] P.-D. Arapoglou, K. Liolis, M. Bertinelli, A. Panagopoulos, P. Cottis, and R. De Gaudenzi, "MIMO over satellite: A review", *IEEE communications surveys & tutorials*, vol. 13, no. 1, pp. 27–51, 2010.
- [5] L. You, K.-X. Li, J. Wang, X. Gao, X.-G. Xia, and B. Ottersten, "Massive MIMO transmission for LEO satellite communications", *IEEE J. Sel. Areas Commun.*, vol. 38, no. 8, pp. 1851–1865, 2020.
- [6] A. Guidotti and A. Vanelli-Coralli, "Clustering strategies for multicast Beamforming in multibeam satellite systems", *Int. J. Satell. Commun. Network.*, vol. 38, no. 2, pp. 85–104, 2020.
- [7] —, "Design trade-off analysis of Beamforming multi-beam satellite communication systems", in *2021 IEEE Aerospace Conference (SOI00)*, 2021, pp. 1–12.
- [8] —, "Geographical scheduling for multicast Beamforming in multi-beam satellite systems", in *2018 9th Advanced Satellite Multimedia Systems Conference and the 15th Signal Processing for Space Communications Workshop (ASMS/SPSC)*, 2018, pp. 1–8.
- [9] M.R. Dakkak, D. G. Riviello, A. Guidotti, A. Vanelli-Coralli, "Evaluation of multi-user multiple-input multiple-output digital beamforming algorithms in B5G/6G low Earth orbit satellite systems", in *Int. J. Satell. Commun. Network.*, pp. 1–17, 2023.
- [10] B. Ahmad, D. G. Riviello, A. Guidotti and A. Vanelli-Coralli, "Graph-Based User Scheduling Algorithms for LEO-MIMO Non-Terrestrial Networks," *2023 Joint European Conference on Networks and Communications & 6G Summit (EuCNC/6G Summit)*, Gothenburg, Sweden, 2023, pp. 270–275.
- [11] M. Y. Abdelsadek, G. K. Kurt and H. Yanikomeroglu, "Distributed Massive MIMO for LEO Satellite Networks," in *IEEE Open J. Commun. Soc.*, vol. 3, pp. 2162–2177, 2022.
- [12] M. Y. Abdelsadek, G. Karabulut-Kurt, H. Yanikomeroglu, P. Hu, G. Lamontagne and K. Ahmed, "Broadband Connectivity for Handheld Devices via LEO Satellites: Is Distributed Massive MIMO the Answer?," in *IEEE Open J. Commun. Soc.*, vol. 4, pp. 713–726, 2023.
- [13] P. Rocca, M. D'Urso and L. Poli, "Advanced Strategy for Large Antenna Array Design With Subarray-Only Amplitude and Phase Control," in *IEEE Antennas Wirel. Propag. Letters*, vol. 13, pp. 91–94, 2014.
- [14] L. Manica, P. Rocca, and A. Massa, "Design of subarrayed linear and planar array antennas with SLL control based on an excitation matching approach," *IEEE Trans. Antennas Propag.*, vol. 57, no. 6, pp. 1684–1691, Jun. 2009.
- [15] Yang, J.; Liu, X.; Tu, Y.; Li, W.; "Robust Adaptive Beamforming Algorithm for Sparse Subarray Antenna Array Based on Hierarchical Weighting", *Micromachines* 2022, 13, 859.
- [16] Y. Aslan, J. Puskely, A. Roederer and A. Yarovsky, "Active Multiport Subarrays for 5G Communications," *2019 IEEE-APS Topical Conference on Antennas and Propagation in Wireless Communications (APWC)*, 2019, pp. 298–303.
- [17] R. J. Mailloux, "Subarray technology for time delayed scanning arrays," in *2009 IEEE International Conference on Microwaves, Communications, Antennas and Electronics Systems*, Tel Aviv, Israel, 2009.
- [18] M. R. Dakkak, D. G. Riviello, A. Guidotti and A. Vanelli-Coralli, "Evaluation of MU-MIMO Digital Beamforming Algorithms in B5G/6G LEO Satellite Systems," *2022 11th Advanced Satellite Multimedia Systems Conference and the 17th Signal Processing for Space Communications Workshop (ASMS/SPSC)*, 2022, pp. 1–8.
- [19] M. R. Dakkak, D. G. Riviello, A. Guidotti and A. Vanelli-Coralli, "Assessment of Beamforming Algorithms with Subarrayed Planar Arrays for B5G/6G LEO Non-Terrestrial Networks", *European Wireless 2023; 28th European Wireless Conference*, Rome, Italy, 2023.
- [20] A. Guidotti, A. Vanelli-Coralli and C. Amatetti, C., "Federated Cell-Free MIMO in Non-Terrestrial Networks: Architectures and Performance", arXiv preprint arXiv:2302.00057, 2023, submitted to IEEE Access. Available online: <https://arxiv.org/abs/2302.00057>.
- [21] ITU-R Radiocommunication Sector of ITU, "Modelling and simulation of IMT networks and systems for use in sharing and compatibility studies (M.2101-0)", Feb. 2017.
- [22] G. Alfano, C.-F. Chiasserini, A. Nordio and D. G. Riviello, "A Random Matrix Model for mmWave MIMO Systems". *Acta Phys. Pol. B*, vol. 51, no. 7, pp. 1627–1640, 2020.
- [23] 3GPP, "TR 38.811 "Study on New Radio (NR) to support non-terrestrial networks (Release 15)". Sep. 2020.
- [24] R. Muharar, J. Evans, "Downlink Beamforming with Transmit-side Channel Correlation: A Large System Analysis," in *IEEE Int. Conf. on Commun. (ICC)*, Jun. 2011.